Desalination and Water Treatment
www.deswater.com
29 (2011) 285–293
May
1944-3994 / 1944-3986 © 2011 Desalination Publications. All rights reserved.
doi: 10.5004/dwt.2011.1494

An expert model for the prediction of water gases thermodynamic properties

S.M. Hosseini[a], F. Parvizian[a]*, A.R. Moghadassi[a]*, A. Sharifi[b], M. Adimi[b], S.J. Hashemi[c]

[a]*Department of Chemical Engineering, Faculty of Engineering, Arak University, P.O. Box 38156-875, Arak, Iran*
Tel./Fax +98 (861) 4173447 ext. 5404; email: Fahime_Parvizian@yahoo.com; A_Moghadassi@yahoo.com
[b]*Department of Chemical Engineering, Faculty of Engineering, Farahan Branch of Islamic Azad University, Farahan, Iran*
[c]*Petroleum University of Technology and Islamic Azad University Ahvaz branch, Ahvaz, Iran*

Received 20 August 2009; Accepted in revised form 20 December 2010

ABSTRACT

Knowledge of the thermodynamic properties of water is necessary for the interpretation of physical and chemical processes. In the current research a new method based on artificial neural network (ANN) was applied for the prediction of water gases thermodynamic properties. The required data were collected and after pre-treating was used for training of ANN. Also the accuracy and trend stability of the trained networks were tested by it generalization ability in predicting of unseen data. The back-propagation learning algorithm, with different training methods such as scaled conjugate gradient (SCG), Levenberg–Marquardt (LM), gradient descent with momentum (GDM), variable learning rate back propagation (GDA) and resilient back propagation (RP) were used for the purpose. The SCG with seven neurons in the hidden layer showed the best performance with minimum mean square error of 0.0001517. Finally, ANN model performance was compared with classical thermodynamical models for the specific volume prediction of superheated water. Some equations of state such as Lee Kesler, NRTL, Soave–Redlich–Kwong and Peng–Robinson were used for the purpose. The comparisons showed the ANN capability for prediction of the thermodynamic properties of water gases.

Keywords: Thermodynamic properties, Water gases; Prediction; Artificial neural network; Equation of state

1. Introduction

The thermodynamic properties of water are important factor to study the mentioned processes [1]. Experimental activities can not be enough to achieve a clear picture of the condition and possible problems as widely doing the experiments, besides involving high costs, is impossible in some cases. Therefore a model with a reasonable accuracy is proposed to predict the required data instead of doing more experiments. The major processes found in chemical engineering are unfortunately nonlinear processes, and previously mentioned approaches fail to respond correctly because of process nonlinearity [2]. ANN is a model that attempts to mimic simple biological learning processes and simulate specific functions of human nervous system [3]. This model creates a connection between input and output variables and keeps underlying complexity of the process inside the system. The ability to learn the behavior of the data generated by a system is the neural network's versatility and privilege [4]. Fast response, simplicity, and capacity to learn are the advantages of ANN compared to classical methods.

This model has been widely applied to predict the physical and thermodynamic properties of chemical com-

* Corresponding author.

pounds. Recently, ANN has been used to predict some pure substances and petroleum fraction's properties [5], activity coefficients of isobaric binary systems [6], thermodynamic properties of refrigerants [3,7–9], and activity coefficient ratio of electrolytes in amino acid's solutions [10], etc. Using the ANN to predict the thermodynamic properties of superheated water instead of approximate and complex analytical equations are the main focus of the current research. Finally, the ability of this model in prediction of water gases thermodynamic properties was valuated in comparison with some equations of state by using unseen data and with the help of experiment data.

2. Artificial neural networks

In order to find relationship between the input and output data derived from experimental work, a more powerful method than the traditional ones are necessary. ANN is an especially efficient algorithm to approximate any function with finite number of discontinuities by learning the relationships between input and output vectors [3,5,11]. These algorithms can learn from the experiments, and also are fault tolerant in the sense that they are able to handle noisy and incomplete data. The ANNs are able to deal with non-linear problems, and once trained can perform prediction and generalization rapidly [12]. They have been used to solve complex problems that are difficult to be solved if not impossible by conventional approaches, such as control, optimization, pattern recognition, classification [3,7].

Artificial neural networks are biological inspirations based on the various brain functionality characteristics. They are composed of many simple elements called neurons that are interconnected by links and act like axons to determine an empirical relationship between the inputs and outputs of a given system. Multiple layers arrangement of a typical interconnected neural network is shown in Fig. 1. It consists of an input layer, an output layer and one hidden layer with different roles. Each connecting line has an associated weight. ANNs are trained by adjusting these input weights (connection weights), so that the calculated outputs may be approximated by the desired values. The output from a given neuron is calculated by applying a transfer function to a weighted summation of its input to give an output, which can serve as input to other neurons, as follows [3,13]:

$$\alpha_{jk} = F_k\left(\sum_{i=1}^{N_{k-1}} w_{ijk}\alpha_{i(k-1)} + \beta_{jk}\right) \tag{1}$$

where α_{jk} is neuron j's output from k's layer β_{jk} is the bias weight for neuron j in layer k. The model fitting parameters w_{ijk} are the connection weights. The nonlinear activation transfer functions F_k may have many different forms. The classical ones are threshold, sigmoid, Gaussian and linear function, etc. [2,3,13–15].

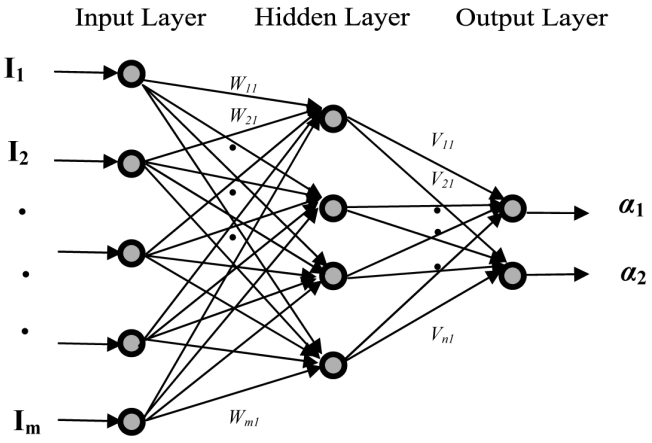

Fig. 1. Schematic of typical multi-layer neural network model.

The training process requires a proper set of data i.e. input (I_i) and target output (t_i). During training the weights and biases of the network are iteratively adjusted to minimize the network performance function [16]. The typical performance function that is used for training feed forward neural networks is the network mean squares errors (MSE) Eq. (2) [2,3,17]:

$$\text{MSE} = \frac{1}{N}\sum_{i=1}^{N}(e_i)^2 = \frac{1}{N}\sum_{i=1}^{N}(t_i - \alpha_i)^2 \tag{2}$$

Also another statistical parameters as RMSE was used to show the accuracy of the ANN model. The RMSE is defined as follows [18]:

$$\text{RMSE} = \sqrt{\frac{\sum_{i=1}^{N}(t_i - \alpha_i)^2}{N}} \tag{3}$$

where t_i and α_i are the experiment and predicted data value respectively. N is the number of used data.

There are many different types of neural networks, differing by their network topology and/or learning algorithm. In the current research, the back propagation learning algorithm, which is one of the most commonly used algorithms, is designed to predict the thermodynamic properties of water. Back propagation is a multilayer feed-forward network with hidden layers between the input and output [2,3,17,19]. The simplest implementation of back propagation learning is the network weights and biases updates in the direction of the negative gradient that the performance function decreases most rapidly. An iteration of this algorithm can be written as follows [2,3,13,17,19]:

$$x_{k+1} = x_k - l_k g_k \tag{4}$$

The process details flowchart to find the optimal model is shown in Fig. 2. There are various back propaga-

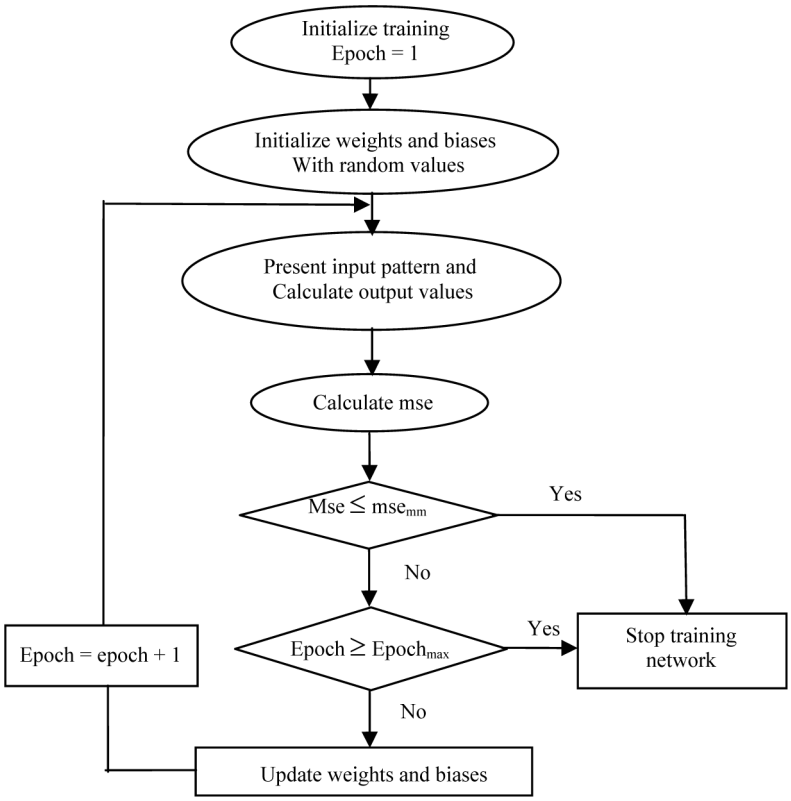

Fig. 2. A training process flowchart.

tion algorithms such as scaled conjugate gradient (SCG), Levenberg–Marquardt (LM), gradient descent with momentum (GDM), variable learning rate back propagation (GDA) and resilient back propagation (RP). LM is the fastest training algorithm for networks of moderate size and it has the memory reduction feature to be used when the training set is large. One of the most important general purpose back propagation training algorithms is SCG [2,3,14,16,17,19].

The neural nets learn to recognize the patterns of the data sets during the training process. Neural nets teach themselves the patterns of the data set letting the analyst to perform more interesting flexible work in a changing environment [3]. Although, neural network may take some time to learn a sudden drastic change, but it is excellent to adapt constantly changing information. However programmed systems are constrained by designed situation and they are not valid. Neural networks build informative models. Because of handling very complex interactions, the neural networks can easily model data, which are too difficult to model traditionally (inferential statistics or programming logic). Performance of neural networks is at least as good as classical statistical modeling, and even better in most cases [19]. Neural networks operate well with modest computer hardware. Although neural networks are computationally intensive, the routines have been optimized to the point that they can now run in reasonable time on personal computers [3]. They do not require supercomputers as they did in the early days of neural network research.

3. Thermodynamic models used [20]

3.1. Soave–Redlich–Kwong (SRK) equation of state

Introduced in 1949 the Redlich–Kwong equation of state was a considerable improvement over other equations of the time. It is still of interest primarily due to its relatively simple form. While superior to the Van-der Waals equation of state, it performs poorly with respect to the liquid phase and thus cannot be used for accurately calculating vapor–liquid equilibria. However, it can be used in conjunction with separate liquid–phase correlations for this purpose.

$$p = \frac{RT}{V_m - b} - \frac{a}{\sqrt{T}V_m\left(V_m + b\right)} \tag{5}$$

$$a = \frac{0.42748R^2T_c^{2.5}}{p_c} \tag{6}$$

$$b = \frac{0.08662RT_c}{p_c} \tag{7}$$

The Redlich–Kwong equation is adequate for calculation of gas phase properties when the ratio of the pressure to the critical pressure (reduced pressure) is less than about one-half of the ratio of the temperature to the critical temperature (reduced temperature):

$$\frac{p}{p_c} \prec \frac{T}{2T_c} \tag{8}$$

In 1972 Soave replaced the $a/\sqrt{(T)}$ term of the Redlich–Kwong equation with a function α (T, ω) involving the temperature and the acentric factor. A function was devised to fit the vapor pressure data of hydrocarbons and the equation does fairly well for these materials.

$$p = \frac{RT}{V_m - b} - \frac{\alpha a}{V_m\left(V_m + b\right)} \tag{9}$$

$$\alpha = \left[1 + \left(0.48508 + 1.55171\omega - 0.15613\omega^2\right)\left(1 - T_r^{0.5}\right)\right]^2 \tag{10}$$

$$T_r = \frac{T}{T_c} \tag{11}$$

ω is the acentric factor for the species. Note especially that this replacement changes the definition of a slightly, as the T_c is now to the second power.

3.2. Peng–Robinson (PR) equation of state

The Peng–Robinson equation was developed in 1976 in order to satisfy the following goals: The parameters should be expressible in terms of the critical properties and the acentric factor. The model should provide reasonable accuracy near the critical point, particularly for calculations of the compressibility factor and liquid density. The mixing rules should not employ more than a single binary interaction parameter, which should be independent of temperature pressure and composition. The equation should be applicable to all calculations of all fluid properties in natural gas processes.

$$p = \frac{RT}{V_m - b} - \frac{a\alpha}{V_m^2 + 2bV_m - b^2} \tag{12}$$

$$a = \frac{0.45724R^2T_c^2}{p_c} \tag{13}$$

$$b = \frac{0.07780RT_c}{p_c} \tag{14}$$

$$\alpha = \left[1 + \left(0.37465 + 1.54226\omega - 0.26992\omega^2\right)\left(1 - T_r^{0.5}\right)\right]^2 \tag{15}$$

$$T_r = \frac{T}{T_c} \tag{16}$$

In polynomial form:

$$Z^3 - (1 - B)Z^2 + \left(A - 3B^2 - 2B\right)Z - \left(AB - B^2 - B^3\right) = 0 \tag{17}$$

$$A = \frac{a\alpha P}{R^2T^2} \tag{18}$$

$$B = \frac{bP}{RT} \tag{19}$$

where ω is the acentric factor of the species and R is the universal gas constant. For the most part the Peng–Robinson equation exhibits performance similar to the Soave equation, although it is generally superior in predicting the liquid densities of many materials, especially nonpolar ones.

3.3. NRTL equation of state

The NRTL (non-random-two-liquid) equation, proposed by Renon and Prausnitz in 1968, is an extension of the original Wilson equation. It uses statistical mechanics and the liquid cell theory to represent the liquid structure. These concepts, combined with Wilson's local composition model, produce an equation capable of representing VLE, LLE, and VLLE phase behavior. Like the Wilson equation, the NRTL model is thermodynamically consistent and can be applied to ternary and higher order systems using parameters regressed from binary equilibrium data. The NRTL model has accuracy comparable to the Wilson equation for VLE systems. The NRTL combines the advantages of the Wilson and van Laar equations. Also it is an activity coefficient model that correlates the activity coefficients γ with the composition of a mixture of chemical compounds, expressed by mole fractions x. For a binary mixture the following equations are used:

$$\ln\gamma_1 = x_2^2\left[\tau_{21}\left(\frac{G_{21}}{x_1 + x_2G_{21}}\right)^2 + \frac{\tau_{12}G_{12}}{\left(x_2 + x_1G_{12}\right)^2}\right] \tag{20}$$

$$\ln\gamma_2 = x_1^2\left[\tau_{12}\left(\frac{G_{12}}{x_2 + x_1G_{12}}\right)^2 + \frac{\tau_{21}G_{21}}{\left(x_1 + x_2G_{21}\right)^2}\right] \tag{21}$$

With

$$\ln G_{12} = -\alpha_{12}\tau_{12} \tag{22}$$

and

$$\ln G_{21} = -\alpha_{12}\tau_{21} \tag{23}$$

τ_{12} and τ_{21} as well as α_{12} are suitable parameters. In most cases the parameters τ:

$$\tau_{12} = \frac{\Delta g_{12}}{RT} \tag{24}$$

and

$$\tau_{21} = \frac{\Delta g_{21}}{RT} \tag{25}$$

are scaled with the gas constant and the temperature and then the parameters Δg_{12} and Δg_{21} are fitted. The NRTL parameters are fitted to activity coefficients that have been derived from experimentally determined phase equilibrium data (vapor–liquid, liquid–liquid, and solid–liquid) as well as from heats of mixing.

3.4. Lee–Kesler (LK) equation of state

The Lee–Kesler correlation is a three parameter corresponding state method for estimating thermodynamic properties of pure, non-polar fluids. For the compressibility factor *Z*, it takes the form:

$$Z = Z_0 + \omega Z_1 \tag{26}$$

where Z_0 is the compressibility factor for fluids of nearly spherical molecules ω is Pitzer's acentric factor and Z_1 corrects for non-spherical intermolecular forces. Tables and charts provide values of Z_0 and Z_1, from which *Z* and, hence, the molar volume can compute. At sub critical temperatures, Z_1 is typically negative ($Z_1 < 0$), indicating that attractive forces dominate the non-spherical contribution to *Z*. At supercritical temperature, Z_1 is typically positive ($Z_1 > 0$), indicating the dominance of repulsive forces that arise when molecules collide. Note that simple fluids have $\omega = 0$.

4. Experimental data

Table 1 lists the range of data that are used to model the water properties [20]. The network inputs are temperature and pressure while outputs are the specific volume, enthalpy and entropy.

Table 1
Minimum and maximum of data used to train the neural network (Perry, 1999)

Superheated vapor region		
Properties	min	max
Temperature, °C	50	1300
Pressure, kPa	10	50000
Specific volume, m^3/kg	0.001503	72.6025
Enthalpy, kJ/kg	1699.51	5409.7
Entropy, kJ/kg K	3.714	11.581

5. Neural network model development

Developing the neural network model to accurately predict thermodynamic properties of water requires its exposure to a large data set during the training phase. The back propagation method with SCG, LM, RP and GDA learning algorithm has been used in feed forward, single hidden layer network. Input layer neurons have no transfer functions. The neurons in the hidden layer perform two tasks: summing the weighted inputs connected to them and passing the result through a non linear activation function to the output or adjacent neurons of the corresponding hidden layer. The computer program has been developed under MATLAB (R2006). Two thirds of data set is used to train each ANN and the rest have been used to evaluate their accuracy and trend stability. The number of the hidden layer neurons is systematically varied to obtain a good estimate of the trained data. The selection criterion is the net output MSE. The MSE of various hidden layer neurons are shown in Fig. 3. As it can be seen the optimum number of hidden layer neurons is determined to be seven for minimum MSE.

Similarly the MSE of various training algorithms are calculated and listed in Table 2 for the obtained seven hidden layer neurons. As Table 2 shows, the Levenberg–Marquardt (LM) and scaled conjugate gradient (SCG) algorithms have the minimum MSE.

Now the trained ANN models are ready to be tested and evaluated against the new data. Table 3 lists the various MSE of the network testing. According to this table the scaled conjugate gradient (SCG) algorithm is the most suitable algorithm with the minimum MSE. Consequently, SCG provides the best minimum error average for both training and testing of the network. Fig. 4

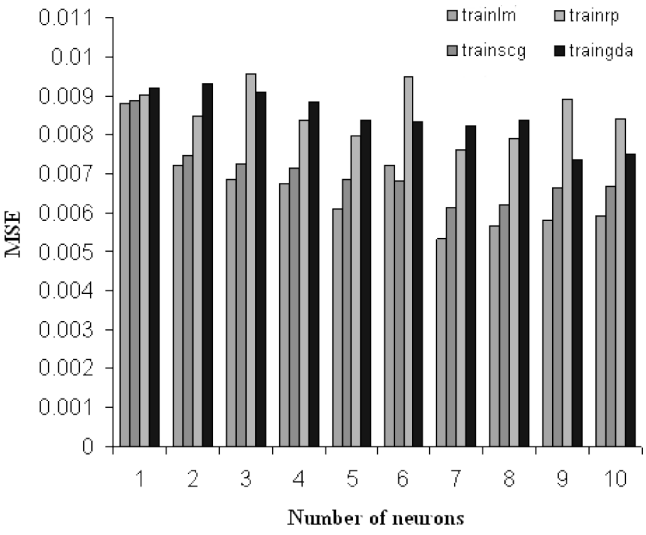

Fig. 3. Determining the optimum number of neurons for some algorithms.

Table 2
MSE comparison between different algorithms to ANN training

Algorithm	MSE of network training
trainlm	0.005835
trainscg	0.005668
trainrp	0.007897
traingda	0.008218
traingdm	0.008806

Table 3
MSE comparison of different algorithms to ANN testing

Algorithm	MSE of network testing
trainlm	0.02752000
trainscg	0.00006794
trainrp	0.01106300
traingda	0.00729000
traingdm	0.00114900

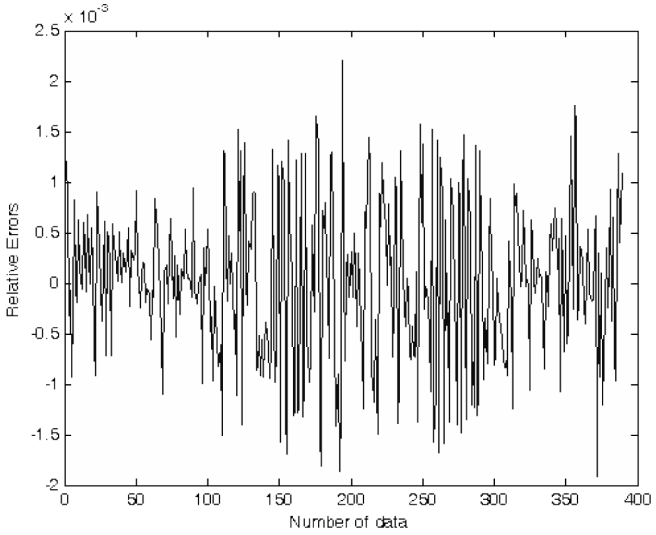

Fig. 4. The relative errors between predicted data by ANN and experimental data; superheated water.

shows the SCG algorithm relative error fluctuations for superheated water.

A scatter plot of typically measured experimental data against the ANN model predictions was shown in Fig. 5. It is obvious from this figure that the ANN provides results very close to process measurements. The predictions which match measured values should fall on the diagonal line. Almost all data lay on this line, which confirms the accuracy of the ANN model. ANN's results

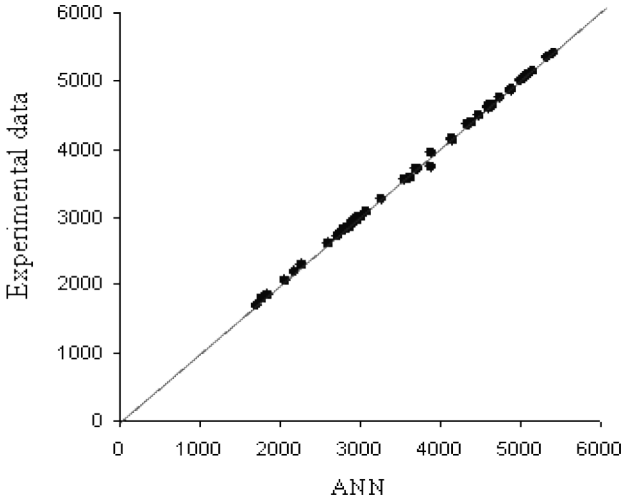

Fig. 5. Evaluation of ANN performance; a scatter plot of typically measured experimental data against the ANN model for unseen data.

showed acceptable estimation performance for prediction of the water properties.

6. Results and discussion

The results show that the ANN predicts water properties very close to the experimentally measured ones. Fig. 6 shows the scatter diagrams that compare the experimental data versus the computed neural network data (enthalpy, entropy and specific volume) over the full range of operating conditions. As it may be seen, a tight cloud of points about the 45° line is obtained for the new data points. This indicates an excellent agreement between the experimental and the calculated data.

To check the performance of ANN model, its estimation ability was compared with some classical thermodynamic models such as Lee–Kesler, NRTL, Soave–Redlich–Kwong and Peng–Robinson. These comparisons for the specific volume of superheated water are shown in Figs. 7–14. Table 4 shows also the RMSE for the used best network in thermodynamic properties predicting.

The results show that NRTL equation of state in high pressure has variation than experimental data. Fig. 15 shows the average relative errors of ANN simulations and equation of state calculations.

7. Conclusion

The ability of ANN to model and predict the superheated water properties have been investigated in this work. The MSE based analysis of the results, are used to verify the suggested approach. The results show a good agreement between experimental data and those predicted by ANN. It has been clearly shown that of the

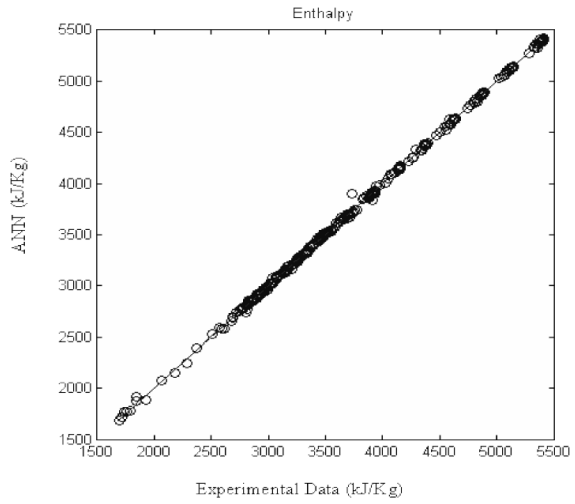

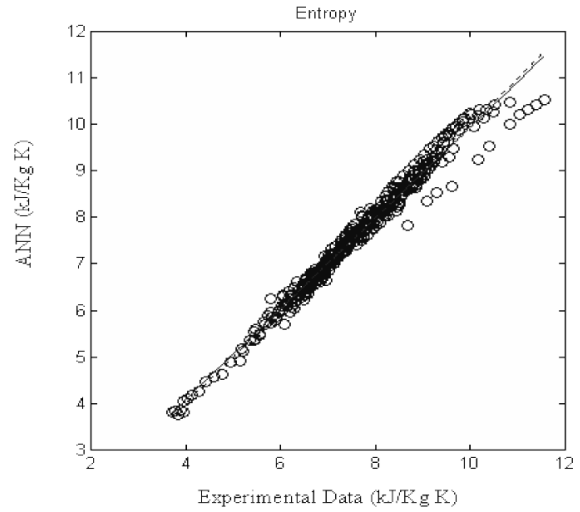

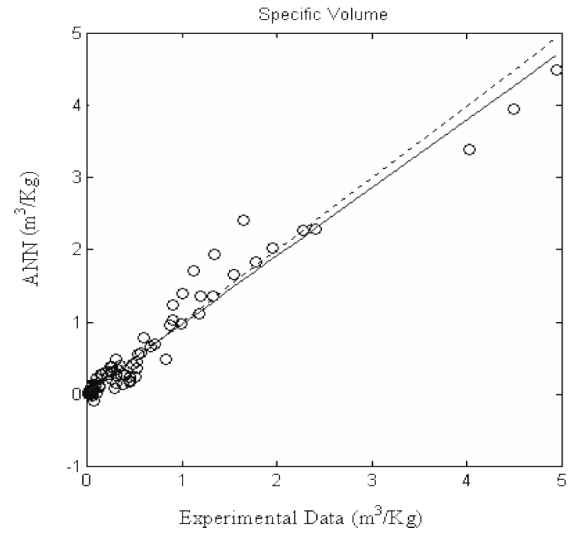

Fig. 6. A comparison between ANN and experimental data for the superheated water.

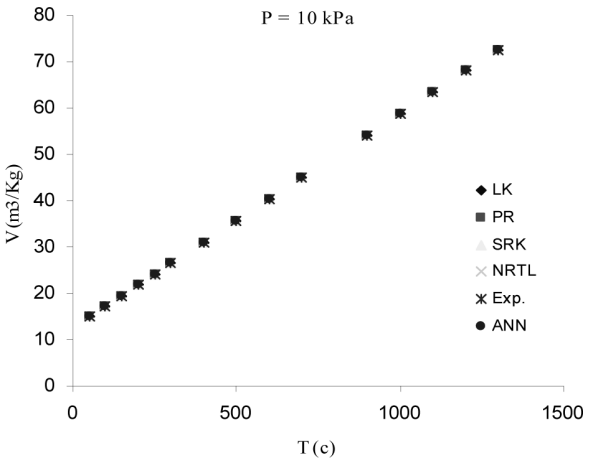

Fig. 7. Comparison between ANN, experimental data and thermodynamic model results for volume of water (P = 10 kPa).

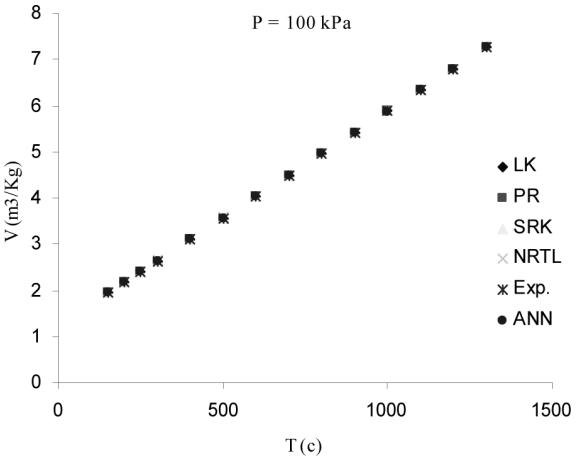

Fig. 8. Comparison between ANN, experimental data and thermodynamic models results for volume of water (P = 100 kPa).

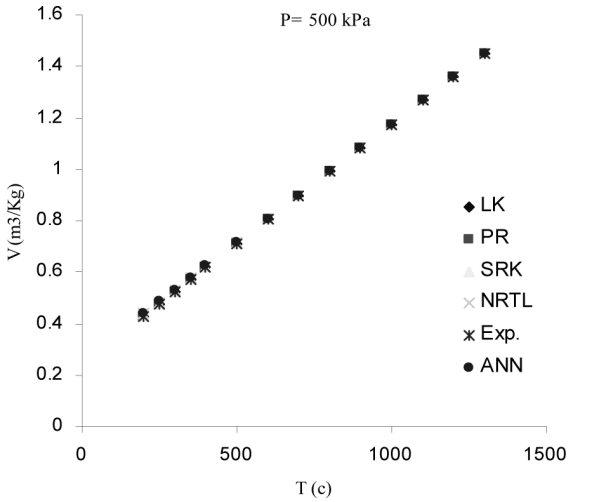

Fig. 9. Comparison between ANN, experimental data and thermodynamic models results for volume of water (P = 500 kPa).

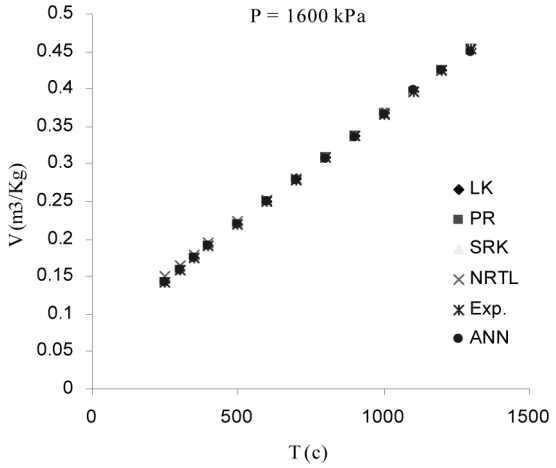

Fig. 10. Comparison between ANN, experimental data and thermodynamic models results for volume of water (P = 1600 kPa).

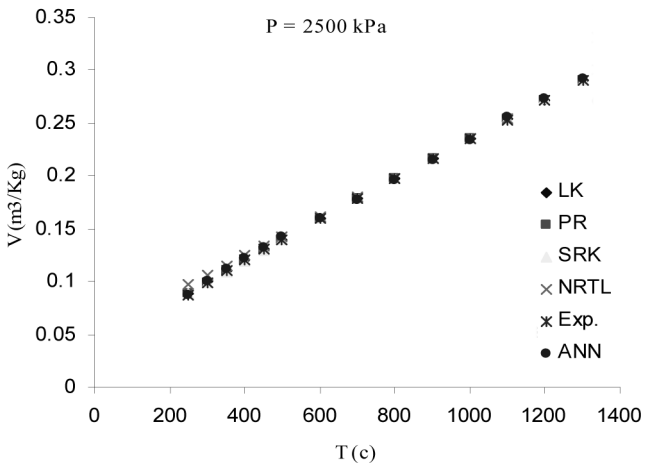

Fig. 11. Comparison between ANN, experimental data and thermodynamic models results for volume of water (P = 2500 kPa).

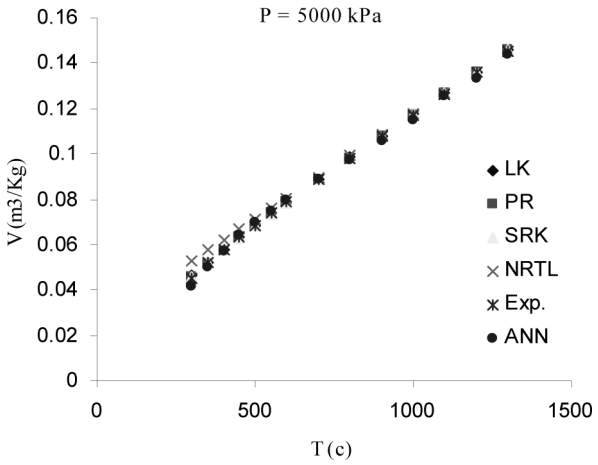

Fig. 12. Comparison between ANN, experimental data and thermodynamic models results for volume of water (P = 5000 kPa).

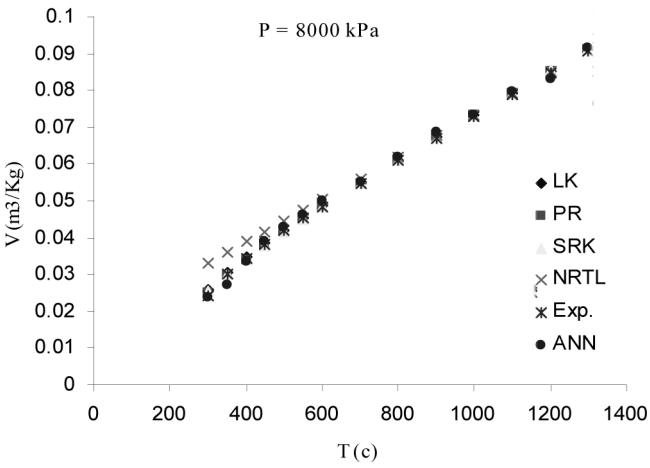

Fig. 13. Comparison between ANN, experimental data and thermodynamic models results for volume of water (P = 8000 kPa).

ANN calculates the water thermodynamic properties based on the experimental data only, instead of using equations of state. Therefore it is not necessary to use approximate and complex analytical equations to calculate water thermodynamic properties.

Acknowledgment

The authors are grateful to Dr. E. Joudaki from Faculty of Chemical Engineering of Arak University for frequent discussion and patient helps during this project.

Symbols

e — Difference between target data and simulation
F — Transfer function
g — Gradient
I — Input data
l — Learning rate
N — Number of data
t — Target data
x — Vector of weights
w — Connection weights

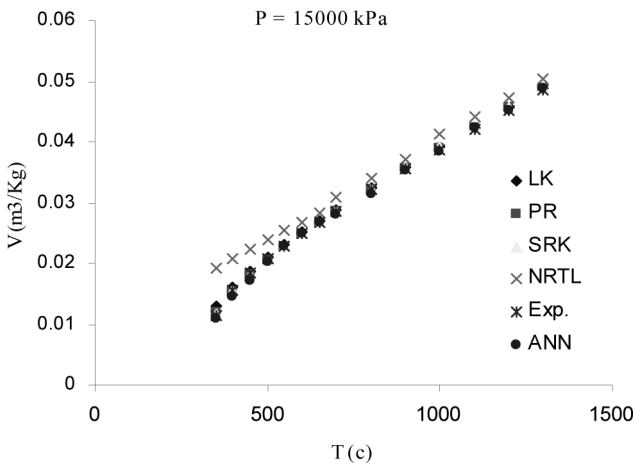

Fig. 14. Comparison between ANN, experimental data and thermodynamic models results for volume of water (P = 15000 kPa).

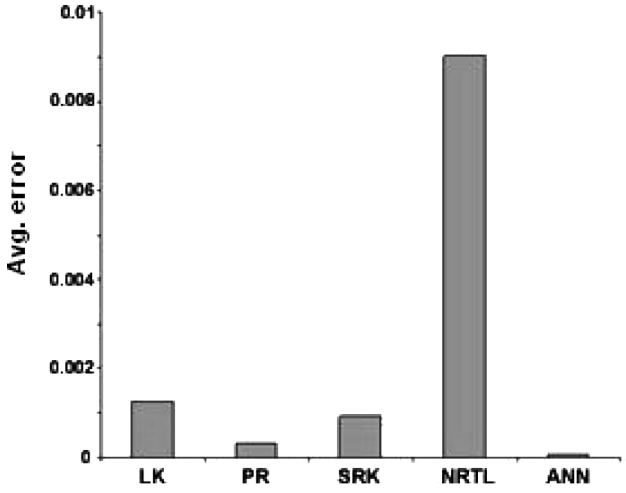

Fig. 15. Comparison between average relative error of ANN and some equations of state.

Table 4
RMSE between experimental and ANN estimated data

Thermodynamic property	RMSE
Specific volume	0.083638
Enthalpy	0.13496
Entropy	0.011937

Greek

α — Output of neuron
β — Bias weight

References

[1] Z. Duan and Z. Zhang, Prediction of the PVT properties of water over wide range of temperature and pressure from molecular dynamics simulation, Physics Earth Planet. Interiors, 149 (2005) 335.
[2] G. Zahedi, A.R. Fazlali, S.M. Hosseini, G.R. Pazuki and L. Sheikhattar, Prediction of asphaltene precipitation in crude oil, J. Petrol. Sci. Eng., 68 (2009) 218.
[3] A.R. Moghadassi, F. Parvizian, S.M. Hosseini and A.R. Fazlali, A new approach for estimation of PVT properties of pure gases based on artificial neural network model, Brazil. J. Chem. Eng., 26(1) (2009) 199.
[4] H.R. Valles, A neural network method to predict activity coefficients for binary systems based on molecular functional group contribution, MSc thesis, University of Puerto Rico, 2006.
[5] R.B. Bozorgmehry, F. Abdolahi and M.A. Moosavian, Characterization of basic properties for pure properties for pure substances and petroleum fractions by neural network, Fluid Phase Equilibria, 231 (2005) 188.
[6] M. Biglin, Isobaric vapor-liquid equilibrium calculations of binary systems using a neural network, J. Serb. Chem. Soc., 69 (2004) 669.
[7] A. Chouai, D. Richon and S. Laugier, Modeling of thermodynamic properties using neural networks application to refrigerants, Fluid Phase Equilibria, 199 (2002) 53.
[8] S. Ganguly, Prediction of VLE data using radial basis function network, Computers Chem. Eng., 27 (2003) 1445.
[9] A. Sozen, E. Arcakilioglu and M. Ozalp, Formulation based on artificial neural network of thermodynamic properties of ozone friendly refrigerant/absorbent couples, Appl. Thermal Eng., 25 (2005) 1808.
[10] M.R. Dehghani, H. Modarress and A. Bakhshi, Modeling and prediction of activity coefficient ratio of electrolytes in aqueous electrolyte solution containing amino acids using artificial neural network, Fluid Phase Equilibria, 244 (2006)153.
[11] M.T. Hagan, H.B. Demuth and M. Beal, Neural Network Design, PWS Publishing Company, Boston, 1996.
[12] A. Sozen, E. Arcakilioglu and M. Ozalp, Investigation of thermodynamic properties of refrigerant /absorbent couples using artificial neural networks, Chem. Eng. Process., 43 (2004) 1253.
[13] R. Gharbi, Estimating the isothermal compressibility coefficient of under saturated Middle East crudes using neural networks, Energy Fuels, 11 (1997) 372.
[14] R.I.W. Lang, A future for dynamic neural networks, Department of Cybernetics, University of Reading, UK, 2000.
[15] A.B. Bulsari, Neural Networks for Chemical Engineers, Amsterdam, Elsevier, 1995.
[16] H. Demuth and M. Beale, Neural Network Toolbox User's Guide, The MathWorks, Inc., 2002.
[17] E. Joudaki, F. Mohammadi, A. Yousefi and T. Mirzazadeh, Prediction of chlor-alkali's caustic current efficiency by artificial neural network; case study: A zero-gap advanced chlor-alkali cell, Desal. Wat. Treat., 8 (2009) 1.
[18] E. Büyükbingol, A. Şişman, M. Akyıldız, F.N. Alpaslan and A. Adejare, Adaptive neuro-fuzzy inference system (ANFIS): A new approach to predictive modeling in QSAR applications: A study of neuro-fuzzy modeling of PCP-based NMDA receptor antagonists, Bioorg. Med. Chem., 15 (2007) 4265–4282.
[19] E.A. Osman and M.A. Al-Marhoun, Using artificial neural networks to develop new PVT correlations for Saudi crude oils, 10th Abu Dhabi International Petroleum exhibition and conference, October 2002.
[20] R.H. Perry, Perry's Chemical Engineer's Handbook, 7th ed., McGrow-Hill, 1999.